Article

# An Activity-based Fluorogenic Probe Enables Cellular and In Vivo Profiling of Carboxylesterase Isozymes

Shi-Yu Liu, Ren-Yu Qu, Rong-Rong Li, Yao-Chao Yan, Yao Sun, Wen-Chao Yang, and Guang-Fu Yang

*Anal. Chem.*, **Just Accepted Manuscript** • DOI: 10.1021/acs.analchem.0c01554 • Publication Date (Web): 08 Jun 2020

# An Activity-based Fluorogenic Probe Enables Cellular and *In Vivo* Profiling of Carboxylesterase Isozymes

Shi-Yu Liu,[†,§] Ren-Yu Qu,[†,§] Rong-Rong Li,[†] Yao-Chao Yan,[†] Yao Sun,[†] Wen-Chao Yang,[*,†] and Guang-Fu Yang[*,†‡]

[†]Key Laboratory of Pesticide & Chemical Biology of Ministry of Education, International Joint Research Center for Intelligent Biosensor Technology and Health, and Chemical Biology Center, College of Chemistry, Central China Normal University, Wuhan 430079, P.R. China

[‡]Collaborative Innovation Center of Chemical Science and Engineering, Tianjin 30071, P.R. China.

[§] These authors made equal contributions.

* Wen-Chao Yang, e-mail: tomyang@mail.ccnu.edu.cn; Tel: 86-27-67867706; Fax: 86-27-67867141; Guang-Fu Yang, e-mail: gfyang@mail.ccnu.edu.cn; Tel: 86-27-67867800; Fax: 86-27-67867141.

## Abstract

Carboxylesterases (CEs) exist as multiple types of isomers in humans, and two major types are CE1 and CE2. They are widely distributed in human tissues and well known for their important roles in drug metabolism and pathology of various diseases. Thus, the detection of CEs in living systems could provide efficient proof in disease diagnostics, as well as important information regarding chemotherapeutic effects of anti-tumor drugs and prognosis. To develop a specific probe to discriminate CEs from other hydrolases, especially cholinesterases, is quite challenging due to their structural similarities and substrate specificity. To date, almost all of the fluorescent probes developed for CEs have been constructed with an acetyl group as the recognition unit. Herein, we proposed a new design strategy of probe-cavity matching, which led to the identification of a new fluorogenic substrate (termed as **HBT-CE**) with high specificity toward both CE isomers and improved sensitivity, considering the higher binding affinity and catalysis efficiency. The promising capability of **HBT-CE** was further demonstrated for endogenous CEs imaging in living cells, zebrafish, and nude mice. In addition, **HBT-CE** was successfully applied in kinetically monitoring of drug-induced CEs regulation in cancer cells. All of these findings suggest that **HBT-CE** is a valuable tool for tracking and imaging endogenous CEs in complex biological systems.


**KEYWORDS** carboxylesterases, fluorescent probe, probe-cavity matching, bioimaging

## INTRODUCTION

Carboxylesterases (EC 3.1.1.1, CEs), including, but not limited to, CE1 and CE2,[1] are capable of hydrolyzing various endogenous and exogenous substrates, such as short- and long-chain acylglycerols, drugs, pesticides and environmental toxicants.[2-4] CEs are known to be classified into five groups[5] and commonly expressed in various animal species.[6] In human, CEs are widely distributed in various tissues, especially in the liver and intestine. Being regulated by various nuclear receptors,[7] CEs play important roles in diseases diagnosis and drug discovery. It has been reported that CEs are up-regulated in pancreatic cancer,[8] neuroblastoma,[9] non-small-cell lung cancer[10] and colorectal cancer[11] tissues. Thus, CEs could serve as important determinants for pharmacokinetics and pharmacodynamics of ester drugs or ester prodrugs, such as irinotecan. Regulation of CEs is also involved in gambogic acid-induced cell apoptosis in cancer cells,[12] CPT-11-related drug resistance,[13] capecitabine-related toxicity[14], and inhibition of tumor growth.[15] Understanding the behavior and regulation of CEs in various diseases is very beneficial for manipulating the disease pathology and clinical drug usage. Interestingly, the abnormal secretion of multiple forms of CEs into serum in diseases, such as acute liver injury[16-17] and acute pancreatitis,[18-19] makes the total content of CE isomers a potential biomarker for the development and/or perpetuation of the above diseases.[20] Therefore, it is essentially important to develop a single method for simultaneous determination of CE isozymes in complex biological systems and physiological events with temporal − spatial resolution.

Among various analysis techniques, fluorescent probes are attractive tools due to their high temporal and spatial resolution.[21-24] Nevertheless, to acquire a highly selective probe for real-time tracking particular target enzyme other than abundant hydrolases and other biological molecules *In Vivo* is quite challenging.[25-27] To date, almost all of the small-molecule-based probe targeting CEs have been constructed with an acetyl group as the recognition group, and most of them incorporate a

hydroxybenzyl moiety-based self-immolative linker.[28-34] In addition, interference from other esterases, including acetylcholinesterase (AChE) and butyrylcholinesterase (BChE), presents a significant challenge due to their overlapping substrate specificities with CEs. However, few of these works discussed the selectivity of the probe for carboxylesterase and cholinesterase in detail.

In this study, we selected 2-(2-hydroxyphenyl) benzothiazole (HBT), a typical excited-state intramolecular proton transfer (ESIPT)-based fluorophore with a large Stokes shift and good biocompatibility,[22] for the construction of a fluorogenic probe (**HBT-CE**) that targets both CE isomers. In addition, the probe has a pivaloyl group, with large steric hindrance, as the recognition unit rather the widely used acetyl group (**Scheme 1)**. This probe exhibits superior selectivity for two cholinesterases, and the mechanism could be explained by analysis of the docking model and determination of the kinetic parameters. Moreover, this new probe shows promising potential for the detection of endogenous CEs in complicated biological systems due to successful bioimaging in cellular and animal models.

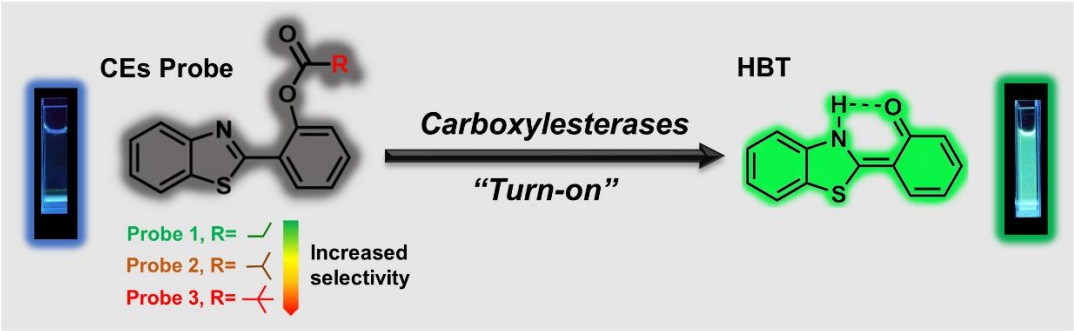


**Scheme 1**. Recognition mechanism of **HBT-CE** toward CEs.

## EXPERIMENTAL SECTION

### Organic Synthesis

**Reagents.** Chemical compounds were of analytical grade and purchased from Sigma-Aldrich (Shanghai, China), and they include bis-p-nitrophenyl phosphate

(BNPP), 4-(2-aminoethyl) benzenesulfonyl fluoride hydrochloride (AEBSF), tacrine, donepezil, sivelestat, fluoxetine, 5-fluorouracil, amino acids (Glu, Thr, Leu, Ser, Ala, Arg, Tyr, Val, Asp, Cys, and Gly), some common inorganic salts (NaCl, $CoCl_2$, $MnCl_2$, $FeCl_3$, KCl, and $CaCl_2$), organic compounds and solvents, 2-(2-hydroxyphenyl) benzothiazole (HBT), propionyl chloride, isobutyryl chloride, pivaloyl chloride, $Et_3N$, dichloromethane (DCM), petroleum ether, and ethyl acetate. CE1 and CE2 were purchased from the Research Institute for Liver Disease (Shanghai, China). Other proteins and enzymes, such as AChE, BChE, carboxypeptidase B (CPB), human serum albumin (HSA), phosphatase, chymotrypsin, and trypsin, were purchased from Sigma-Aldrich. Unless otherwise noted, all of the starting materials were commercially available and treated with standard methods provided by the manufactures' instructions.

**Instrumentation**. Fluorescence spectra were recorded with a microplate reader (SpectraMax M5, Molecular Devices) using 96-well luminescent plates or quartz cuvette (Hellma, Germany). $^1H$ NMR and $^{13}C$ NMR spectra for the target compounds were determined in $CDCl_3$ on a Varian Mercury 500 MHz or 125 MHz spectrometer, and resonances (δ) are given in ppm relative to tetramethylsilane (TMS). High-resolution mass spectrometry (HRMS) was obtained on Agilent 6460 Triple Quadrupole mass spectrometer.

**Synthesis of probes 1-3** A mixture of the 2-(2-hydroxyphenyl) benzothiazole (0.44 mmol, 100 mg), propionyl chloride (0.54 mmol, 50 mg), and $Et_3N$ (0.88 mmol, 89 mg) in THF (3 mL) was stirred at ambient temperature for 1.0 h. The progress of the reaction was monitored by TLC. After the reaction was complete, the mixture was poured into a separatory funnel containing 10 mL 1 M HCl and 10 mL $CH_2Cl_2$. The layers were separated, and the aqueous layer was extracted with $CH_2Cl_2$ (2 × 10 mL). The combined organic layers were dried over $Na_2SO_4$. The extract was concentrated under vacuum, and the residue was purified by chromatography on silica gel using petroleum ether: ethyl acetate = 40: 1 to afford probe **1** as a white solid. Synthesis of probes **2-3** was conducted via the same procedure for **probe 1,** with isobutyryl

chloride or pivaloyl chloride accordingly. The NMR and HRMS data are listed as below.

**Probe 1** (yield 56.2%, 70.1 mg) $^{1}$H NMR (400 MHz, $CDCl_3$) δ 8.32 (d, *J* = 7.8 Hz, 1H), 8.09 (d, *J* = 8.4 Hz, 1H), 7.93 (d, *J* = 8.0 Hz, 1H), 7.55 – 7.47 (m, 2H), 7.45 – 7.35 (m, 2H), 7.25 (d, *J* = 7.8 Hz, 1H), 2.81 (q, *J* = 7.8 Hz, 2H), 1.32 (t, *J* = 7.8 Hz, 3H). $^{13}$C NMR (101 MHz, $CDCl_3$) δ 172.58, 162.59, 152.79, 148.34, 135.28, 131.43, 130.27, 129.35, 126.31, 126.00, 125.34, 123.68, 123.27, 121.32, 28.21, 8.84. HRMS (MALDI): Calcd for $C_{16}H_{13}NO_2S$ $[M+H]^+$ 284.0740. Found: 284.0741.

**Probe 2** (yield 66.6%, 87.2 mg) $^{1}$H NMR (400 MHz, $CDCl_3$) δ 8.26 (d, *J* = 8.0 Hz, 1H), 8.08 (d, *J* = 8.0 Hz, 1H), 7.93 (d, *J* = 8.0 Hz, 1H), 7.55 – 7.48 (m, 2H), 7.44 – 7.35 (m, 2H), 7.21 (d, *J* = 8.0 Hz, 1H), 3.06 – 2.96 (m, 1H), 1.38 (d, *J* = 7.2 Hz, 6H). $^{13}$C NMR (101 MHz, $CDCl_3$) δ 175.26, 162.72, 152.96, 148.53, 135.39, 131.37, 130.40, 126.28, 126.24, 125.29, 123.59, 123.30, 121.34, 34.52, 18.86. HRMS (MALDI): Calcd for $C_{17}H_{15}NO_2S$ $[M+H]^+$ 298.0896. Found: 298.0898.

**Probe 3** (yield 59.9%, 82.1 mg) $^{1}$H NMR (400 MHz, $CDCl_3$) δ 8.16 (d, *J* = 7.2 Hz, 1H), 8.09 (d, *J* = 8.0 Hz, 1H), 7.93 (d, *J* = 7.6 Hz, 1H), 7.54 – 7.48 (m, 2H), 7.43 – 7.34 (m, 2H), 7.14 (d, *J* = 8.0 Hz, 1H), 1.42 (s, 9H). $^{13}$C NMR (101 MHz, $CDCl_3$) δ 176.95, 163.03, 153.19, 148.86, 135.42, 131.40, 130.72, 126.67, 126.24, 126.22, 125.26, 123.57, 123.31, 121.39, 39.23, 27.28. HRMS (MALDI): Calcd for $C_{18}H_{17}NO_2S$ $[M+Na]^+$ 334.0872. Found: 334.0871.

**Cell culture and live cell imaging** Cancer cell lines were purchased from Procell Life Science and Technology Co., Ltd. (Wuhan, China). Human liver hepatocellular cells Hep G2, human ovarian carcinoma cells SKOV3 and human cervical carcinoma cells HeLa were grown in DMEM (Gibco, USA) supplemented with 10% (V/V) fetal bovine serum (Gibco). Human non-small cell lung carcinoma cells A549 were grown in 1640 (Gibco) supplemented with 10% (V/V) fetal bovine serum (Gibco); both cell lines were maintained at 37°C and 5% $CO_2$.

Prior to the cellular imaging experiments, cells were seeded on glass-bottom cell culture dishes (NEST, 15 mm) at a density of around $3 \times 10^5$ cells per well in 2.0 mL

of culture medium. After the cells were washed with PBS, they were preincubated with or without inhibitors (AEBSF, 1 mM or BNPP, 500 μM) for 30 min. Then, **HBT-CE** (20 μM) in DMEM was added to the cells. Fluorescence images were immediately acquired with an inverted fluorescence microscope (Olympus IX71, Japan) every 10 min without any movement. Fluorescence image data were then analyzed by quantifying the fluorescence intensity of each cell using ImageJ software (National Institutes of Health, America). Each experiment included at least three independent biological repeats, and at least 3 images from different fields of view were captured for each well of cells.

**Live imaging in zebrafish.** The zebrafish were provided by Nanjing EzeRinka Biotechnology Co., Ltd. Before the imaging study, the zebrafish were placed in 35 mm confocal dishes and incubated with or without 50 μM tacrine, 500 μM BNPP or 500 μM AEBSF for 30 min. After the medium in each group was replaced with fresh E3 medium, the cells were treated with 20 μM **HBT-CE** and further incubated for 20 min. Fluorescence images were acquired by an inverted fluorescence microscope with a 4× objective lens.

**Live imaging in nude mice.** Nude mice (BALB/c-nu, 5 weeks) were intravenously injected with 200 μL of 200 μM **HBT-CE** using a microinjector for 30 min. Fluorescence images were then acquired with a Lago X *In Vivo* Imaging system (Spectral Instruments Imaging, Arizona, USA) with an excitation laser at 365 nm and an emission filter of 510 nm.

## RESULTS AND DISCUSSIONS

### Probe design and characterization

Broadly speaking, serine hydrolases, including CEs, utilize the same catalytic triad (consisting of amino acid residues His, Asp or Glu and Ser) to carry out nucleophilic attack of amide or ester bonds. Thus, there are two issues for designing a fluorescent

probe for CE detection: the catalytic efficiency of both major CE isomers and the discrimination between CEs and BChE activity. To address these challenges, we analyzed the crystal structures of human BChE (PDB entry: 1P0M)[35] and CE (PDB entry: 1MX5)[36] and proposed a "probe-cavity matching strategy" for the design of a specific CEs probe. More specifically, the better the probe-cavity match, the higher specificity it may achieve. Directed by this strategy, 2-(2'-hydroxyphenyl) benzothiazole (**HBT**) was introduced as the fluorophore, and an alkanoyl moiety was used to quench the fluorescence of HBT. An "off-on" fluorescence signal change could occur when the ester bond was cleaved by the catalysis of CEs and, thus, could illuminate CEs in living system. Three alkanoyl groups with different sizes were introduced as recognition groups for the construction of the target probes, an ethyl group for probe **1**, isopropyl group for probe **2** and tertiary butyl group for probe **3**. The structural characterizations of probes **1-3** are provided in the supplementary material (Figures S1–S6). As shown in Figure S7, the fluorescence signal of probe **3** (termed as **HBT-CE)** was adequately quenched at 460 nm, with excitation at 325 nm. All of the three probes exhibited similar responses against both CEs. More importantly, although the relative activity for sensing CEs decreased with increasing steric hindrance of the recognition group, the specificity of them over the BChE improved and probe **3** showed the best specificity (Figure 1). The inteference of various small molecules including amino acids and metal ions toward **HBT-CE** was also investigated, as shown in Figure S8, the probe shows high selectivity among all these analytes.

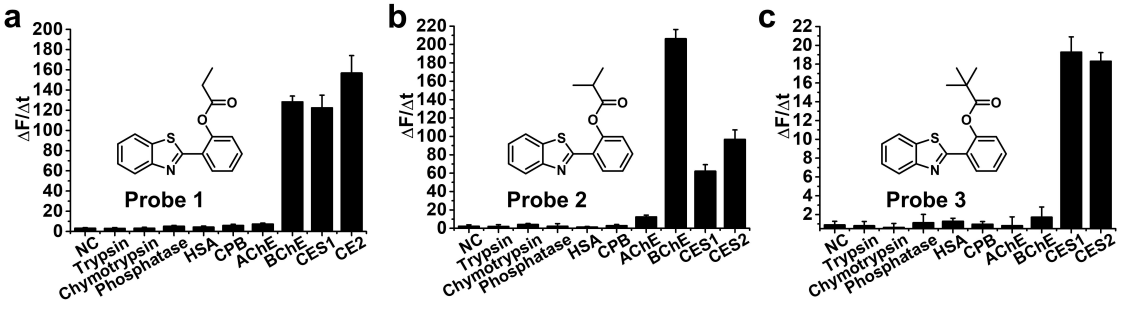


**Figure 1.** Specificity of probe **1** (a), probe **2** (b) and probe **3** (c) (10 μM, 10 min) toward CEs and other hydrolases or proteins in phosphate buffer (10 mM, pH 7.4) at

30℃.The tested hydrolases or proteins include trypsin (10 μg/mL), chymotrypsin (10 μg/mL), phosphatase (10 μg/mL), HSA (10 μg/mL), CPB (10 μg/mL), AChE (10 μg/mL), BChE (10 μg/mL), CE1 (10 μg/mL), and CE2 (10 μg/mL).

To understand the ability of probe **HBT-CE** to discriminate between CE and BChE, we docked this probe into the active sites of both enzymes, respectively. As depicted in Figures 2a and b, **HBT-CE** exhibited a better fit with the CE cavity than that of BChE. In addition, it revealed that the proximity of catalytic Ser1221 to the carbonyl group of **HBT-CE** was around 4.8 Å in CE, whereas the proximity of catalytic Ser198 to the carbonyl group of **HBT-CE** was around 5.9 Å in BChE (Figure 2c and d). This suggests that **HBT-CE** in CE active center is much more susceptible to Ser-triggered nucleophilic attack than that in the BChE active center. Further experiments also confirmed its high selectivity for CEs over other small analytes, such as amino acids and metal ions (Figure S8). The excellent selectivity of the probe implies the efficacy of **HBT-CE** for evaluating CEs activity.

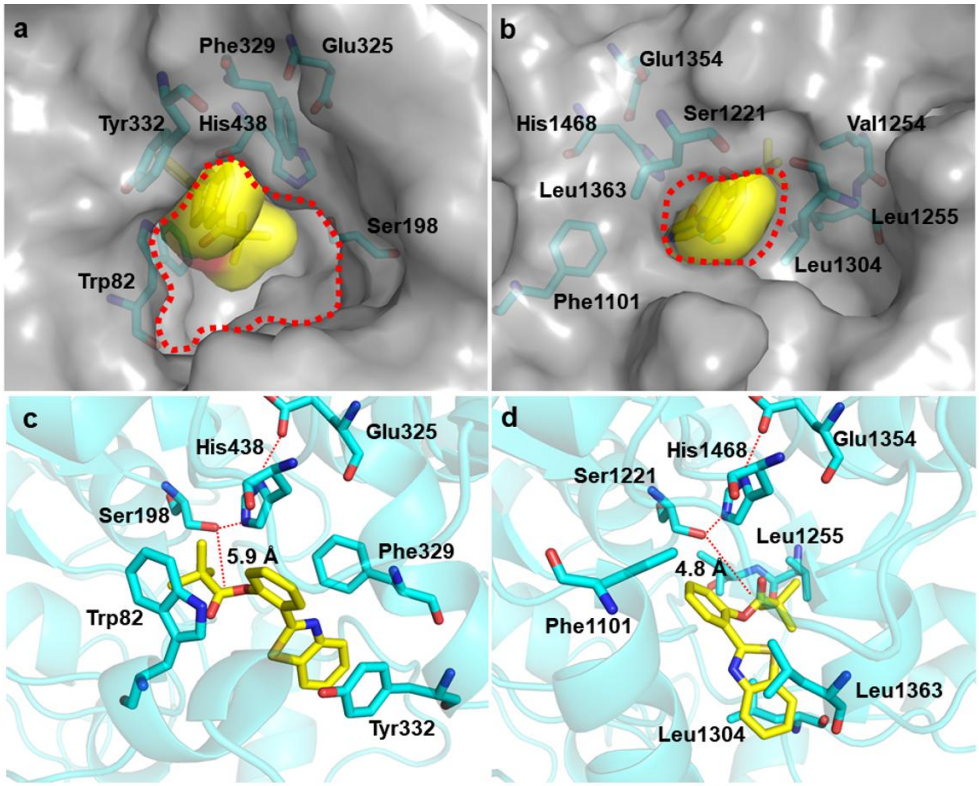


**Figure 2.** Simulated binding models of **HBT-CE** in human BChE (a in sphere type and (c in cartoon type. The simulated binding models of **HBT-CE** in human CE (b in

sphere type and (d in cartoon type. The probe **HBT-CE** is indicated in yellow, and the key residues of the cavities for both enzymes are shown in cyan. Matching between **HBT-CE** and the two enzymes is indicated by red dashed lines, respectively. The red dash lines refer to the catalytic traid, and the distances between the hydroxyl of the catalytic Ser residue and the carbonyl group of **HBT-CE**.

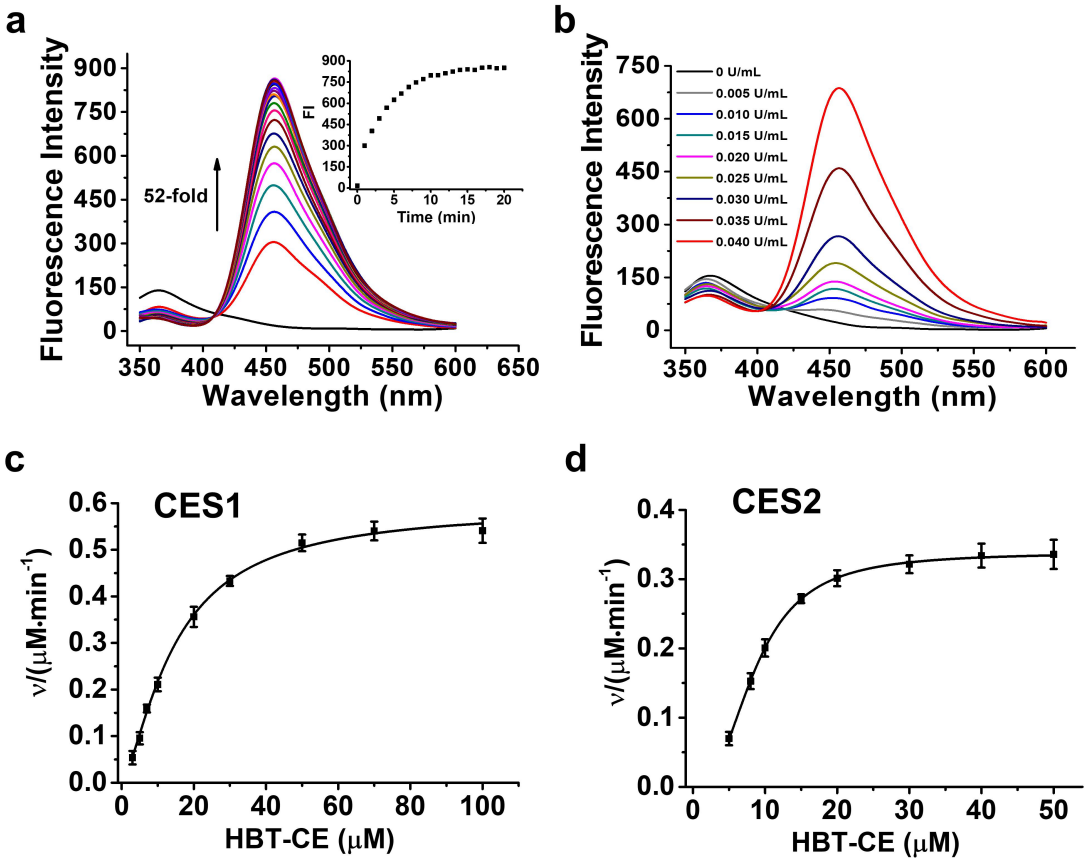


**Figure 3.** Kinetic characterization of **HBT-CE** as a selective substrate for CEs. (a) Time-dependent changes in the fluorescence intensity of **HBT-CE** (10 μM) in the presence of PLE (1 μg/mL). (b) Dose-dependent changes in the fluorescence of **HBT-CE** (10 μM) at various concentrations of PLE (0-0.04 U/mL). (c and d) Michaelis – Menten curve for **HBT-CE** catalysis by CE1 (10 μg/mL) or CE2 (10 μg/mL), the assays were all conducted in phosphate buffer (10 mM, pH 7.4) at 30°C.

We firstly tested the pH-dependent profile of **HBT-CE** catalyzed by CEs in aqueous solution. As shown in Figure S9, the probe showed best performances at

around physiological pH, and thus pH 7.4 was chosen as the *in vitro* test condition prior to the application in biological system. Herein, we chose porcine liver esterase (PLE) as the substitution of multiple CE isomers due to their high substrate similarities.[29] As shown in Figure 3a, the initial fluorescence of **HBT-CE** (10 μM) at 460 nm was adequately quenched, and the FI increased over 52-fold within 20 min at physiological conditions upon the addition of PLE. The enzyme-triggered reaction mechanism was further validated by HPLC analysis and the data was shown in Figure S10. Moreover, the fluorescence response of **HBT-CE** toward various concentrations of PLE was linear, and the limit of detection (LOD) was $4.02 \times 10^{-5}$ U/mL, which indicates that **HBT-CE** is more sensitive than all of the former reported CEs probes (Figures S11 and S12). To quantify the catalytic activity of both CEs against HBT-CE, we characterized the hydrolysis of **HBT-CE** catalyzed by CE1 and CE2, respectively (Figure 3c and d). Accordingly, the Michaelis constants ($K_m$) and the catalytic constants ($k_{cat}$) were determined, and the data are listed in Table 1. Intriguingly, although both kinetic parameters of **HBT-CE** catalyzed by CE1 are around one-fold higher than those catalyzed by CE2, their overall catalytic efficiencies ($k_{cat}/K_m$) were quite similar. This explains why **HBT-CE** exhibits a similar response toward both CE1 and CE2. To compare the catalysis efficiency of **HBT-CE** among the existing CEs probes, we further determined the kinetic parameters of **HBT-CE** toward PLE, as shown in Figures S12 and S13. The $k_{cat}/K_m$ value for **HBT-CE** is 6.4-fold higher than the best performing probe reported recently.[29] The above analysis reveals that **HBT-CE** should be a suitable substrate for both CE1 and CE2 detection in living systems.

**Table. 1.** Kinetics parameters of **HBT-CE** catalyzed by CE1 and CE2, respectively.

| | $K_m$ (μM) | $k_{cat}$ ($s^{-1}$) | $k_{cat}/K_m$ ($M^{-1}\cdot s^{-1}$) |
|---|---|---|---|
| **CE1** | 14.69 ± 2.58 | 3.07 ± 0.19 | ~$2.09\times10^5$ |
| **CE2** | 8.60 ± 0.58 | 1.75 ± 0.07 | ~$2.03\times10^5$ |

## Cellular imaging and kinetic tracking

To illustrate the capability of **HBT-CE** for the specific detection of endogenous CEs in living cells, we first applied **HBT-CE** in Hep G2 cell lysates since the Hep G2 cell line is known to express CEs in high concentrations.[29] As shown in Figure S14, preincubation with AEBSF (serine protease inhibitor) or BNPP (selective inhibitor for carboxylesterases) resulted in fluorescence responses that had declined by over 90%, compared with the cells treated with 0.1% DMSO. In addition, the preincubation with other common esterase inhibitors, such as tacrine (inhibitor for cholinesterase), donepezil (selective inhibitor for AChE) and sivelestat (particular inhibitor for neutrophil elastase), did not change the fluorescence of **HBT-CE**, which primarily demonstrated the potential of **HBT-CE** for bioimaging. Prior to cell image, we firstly tested the cytotoxicity of **HBT-CE** against Hep G2 cells by MTT assay. As depicted in Figure S15, the cell viability of Hep G2 cells treated with the probe after 24 h at various concentration maintained over 80%, which demonstrated the good biocompatibility of **HBT-CE**. Hence, we further adopted **HBT-CE** for kinetic monitoring of CEs in living cells. As displayed in Figure 4a and b, the green fluorescence of cells treated with **HBT-CE** quickly increased and became visible within 10 min. The intracellular fluorescence signal enhanced in a time-dependent manner and plateaued around 40 min. In contrast, no obvious green fluorescence of cells pretreated with 1 mM AEBSF or 500 μM BNPP for 30 min before the addition of **HBT-CE** was observed, which is in good agreement with the cell lysate-based assay. These results suggest that **HBT-CE** could serve as a new tool for imaging of endogenous CEs in living species, with high resolution and sensitivity.

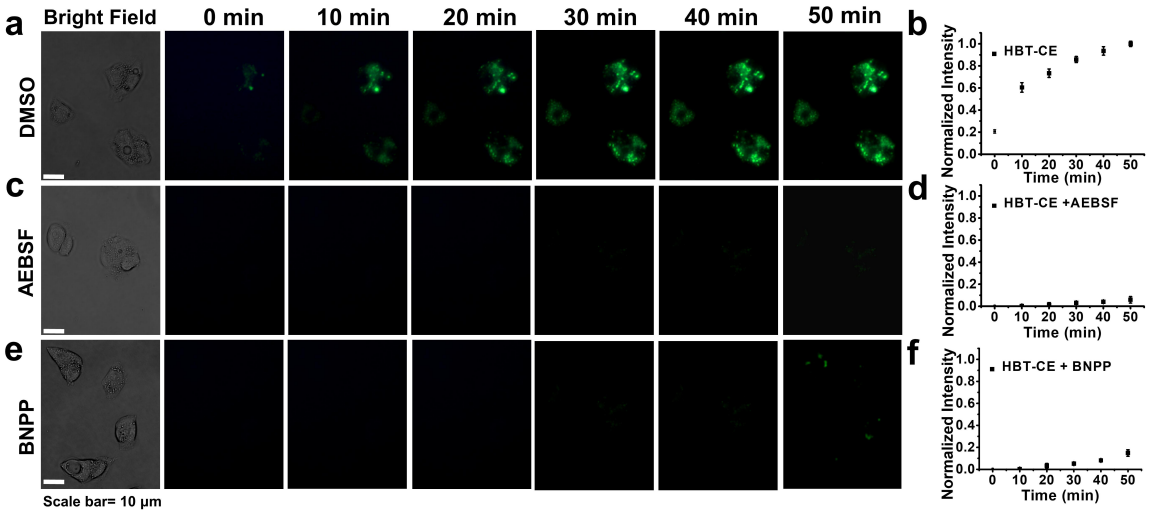


**Figure 4.** Real-time detection of CEs in living Hep G2 cells. (a, c, e) Time-lapse imaging of endogenous CEs in Hep G2 cells using **HBT-CE** (20 μM) without (a) and with pre-incubation of 1 mM AEBSF (c) or 500 μM BNPP (e) for 30 min. (b, d, f) Quantification of the fluorescence intensity of the microscopy images.

To further investigate the subcellular localization of CEs, **HBT-CE** was employed to stain cells, with commercial organelle dyes as references. In general, Hep G2 cells were co-stained with **HBT-CE** and three separate red dyes: ER-tracker red, Mito-tracker red and Lyso-tracker red (Figure 5). Thus, the Pearson correlation coefficient (Rr) was determined to calculate the linear correlation between two color staining methods. From Figure 5, CEs mainly distributed in the endoplasmic reticulum and mitochondria, rather than in lysosomes.

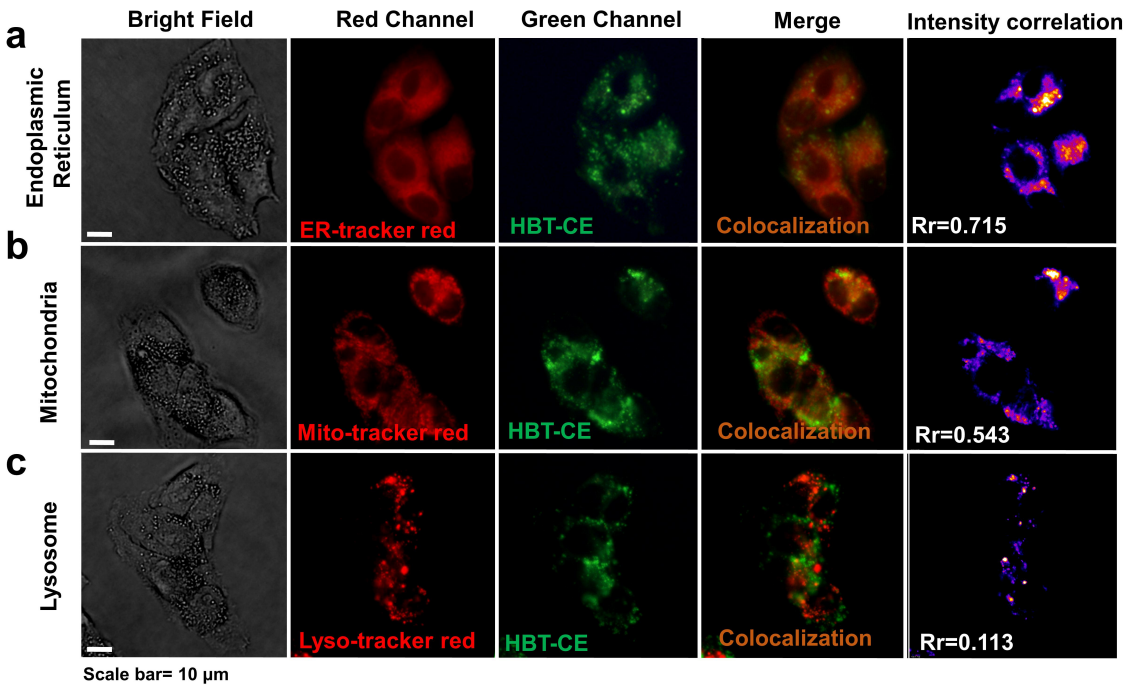


**Figure 5.** Determination of subcellular localization of CEs with **HBT-CE.** (a – c) Co-incubated with **HBT-CE** (20 μM) and commercial organelle trafficking dye ER-tracker red (a, 1 μM), Mito-tracker red (b, 1 μM), and Lyso-tracker red (c, 1 μM). From left to right: Bright-field images; commercial dye images; **HBT-CE** images; merged images of commercial dye and **HBT-CE** images; and pseudo color images indicating the extent of correlation between the intensities of **HBT-CE** and organelle trackers.

The high selectivity of this newly identified probe for CEs monitoring inspired us to extend its application in understanding biological events. As mentioned before, CEs have important roles in drug metabolism and disease pathology;[12, 37-38] thus, identifying the relative content of CEs in different cell lines (especially cancer cell lines) could be useful in predicting the chemotherapeutic effect of anti-cancer drugs and prognosis. First, we employed the **HBT-CE** probe to compare endogenous CEs among various cell lines, including human liver carcinoma cells Hep G2, non-small-cell lung carcinoma cells A549, ovarian carcinoma cells SKOV3, and cervical carcinoma cells HeLa.

As shown in Figures 6a and 6b, the green fluorescence intensity of Hep G2 cells treated with **HBT-CE** is much higher than that of other cancer cell lines. Thus, it was speculated that the CEs content in Hep G2 cells is about 4.1-fold and 9.6-fold that of SKOV3 cells and HeLa cells, respectively. The above result suggests that the metabolism of ester-bond-bearing drugs in HeLa cells may be less efficient, compared with the other three tested cell lines.

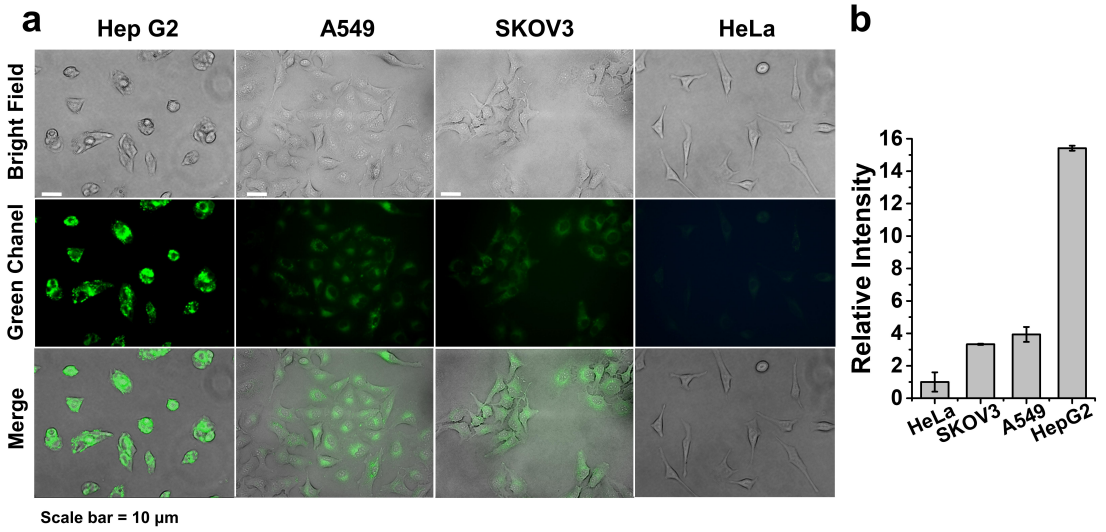


**Figure 6.** Determination of the relative content of endogenous CEs in different cell lines. (a) Fluorescence images taken from different cells (Hep G2, A549, SKOV3, HeLa) incubated with **HBT-CE** (20 μM) for 30 min. (b) Quantification of relative fluorescence intensities from the microscopy images.

Enzyme prodrug approaches are widely adopted in cancer therapy, and the activity of CEs is crucial for the conversion of many prodrugs to their active ingredient, such as irinotecan[37] and capecitabine;[14] thus, an activity-based evaluation of CEs could be more reliable than protein expression level analysis in this aspect. Since extensive research has proved the combination of chemotherapeutic agents could improve anti-tumor drug efficacy,[39-41] the ability to predict the interaction between drugs and CEs could help to instruct the usage

of CEs catalyzed prodrugs. Next, we utilized the **HBT-CE** probe to monitor the kinetic change in CEs in the presence of drug-induced regulation. 5-fluorouracil (5-FU) is a widely used anti-tumor drug that is frequently applied in combinational therapy[42-43] with other chemotherapy agents. Therefore, the interaction between CEs and 5-FU can influence the efficacy of CEs-dependent pro-drugs, such as irinotecan. As shown in Figure 7, treatment with 20 μM 5-fluorouracil significantly induced the up-regulation of CEs activity in Hep G2 cells, whereas the activity of CEs decreased significantly when the cells were treated with fluoxetine, an antidepressant drug that could down-regulate the expression of CEs.[44] These results indicate that 5-FU might promote the conversion of irinotecan to the active metabolite, due to the up-regulation of CEs activity. Thus, the combination of 5-FU and irinotecan could be quite beneficial in cancer therapy.

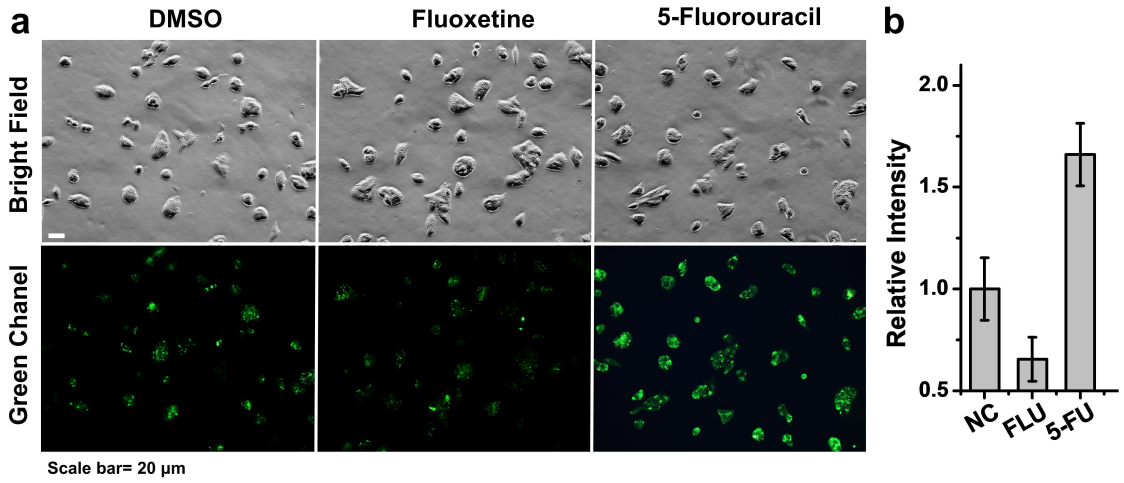


**Figure 7.** Monitoring of drug-induced regulation of CEs in Hep G2 cells by **HBT-CE.** (a) Live imaging fluorescence image taken from Hep G2 cells preincubated with DMSO (0.5%), fluoxetine (25 μM) or 5-fluorouracil (20 μM) for 24 h, followed by incubation with **HBT-CE** (20 μM) for 30 min. (b) Quantification of relative fluorescence intensities from microscopy images.

**Specific detection of CEs in living zebrafish**

To further assess the potential of **HBT-CE** for visualizing CEs *In Vivo*, we performed CEs sensing in an aquatic model organism. Zebrafish are frequently adopted as a model system for fluorescent probe-based bioimaging.[45-47] We applied **HBT-CE** into live image with zebrafish, and strong green fluorescence appeared throughout the zebrafish bodies, including eyes (Figure 8). As a control experiment, zebrafish treated with tacrine prior to the treatment of **HBT-CE** had no obvious effect on the FI signal. However, the fluorescence signal in zebrafish preincubated with CEs specific inhibitor BNPP or serine protease inhibitor AEBSF exhibited a significantly diminished fluorescence signal. The above results demonstrate that **HBT-CE** is a valuable visualizing tool for monitoring CEs activity in living organisms.

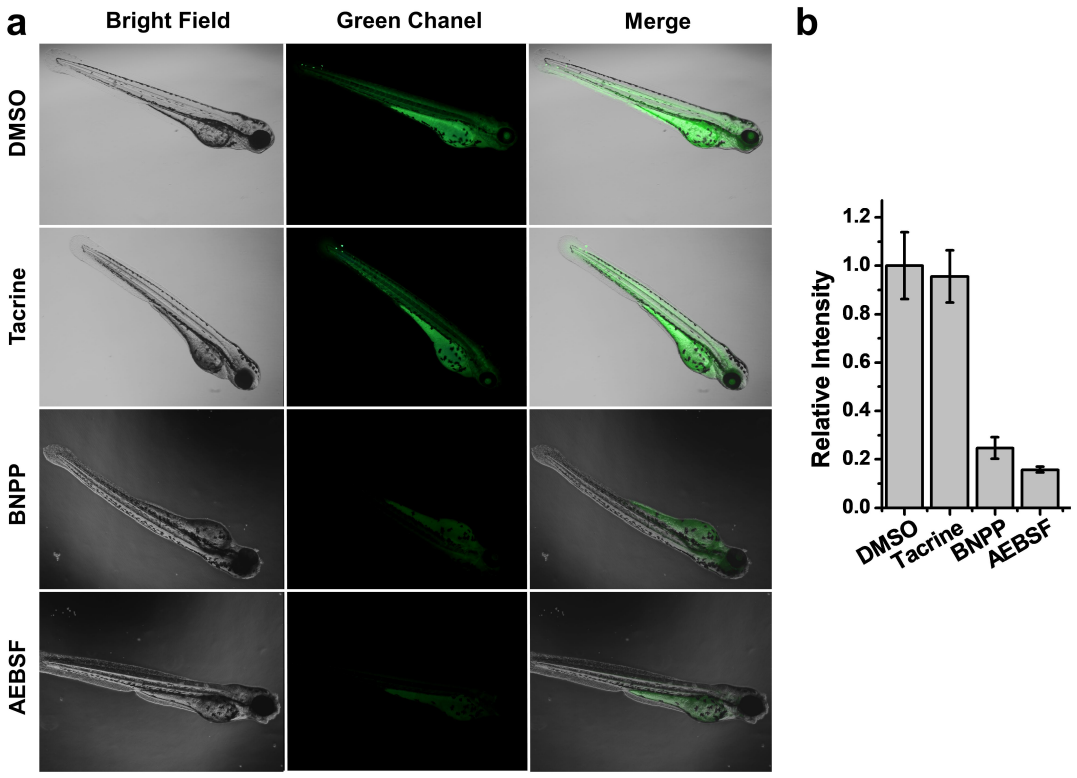


**Figure 8.** *In Vivo* detection of CEs in zebrafish by **HBT-CE.** (a) Live imaging fluorescence image taken from zebrafish preincubated with DMSO (0.5%), Tacrine (50 μM), BNPP (500 μM) or AEBSF (500 μM) for 30 min, followed by incubation with **HBT-CE** (20 μM) for 20 min. (b) Quantification of relative fluorescence intensity from microscopy images.

**Determination of the biodistribution of CEs in tissue of nude mice**

To further investigate the feasibility of **HBT-CE** in detecting CEs in living animals, we applied **HBT-CE** in nude mice via tail vein injection. Although the tissue penetration of **HBT-CE** in live imaging is not sufficient, the remarkable fluorescence signal, however, was clearly observed in the abdomen of a nude mouse, and this is consistent with a previous report (Figure 9a).[48] To obtain more precise biodistribution data of CEs in various organisms, we dissected major organs for *in-situ* imaging. As shown in Figure 9b, the fluorescence signal was mainly localized in the small intestine, liver and lung, and no signal was detected in the heart, kidney and spleen. Although the tissue distribution of CEs has already been well studied via the Northern blot assay,[49] the **HBT-CE** probe provides a fast and efficient method for evaluating CEs biodistribution in living samples.

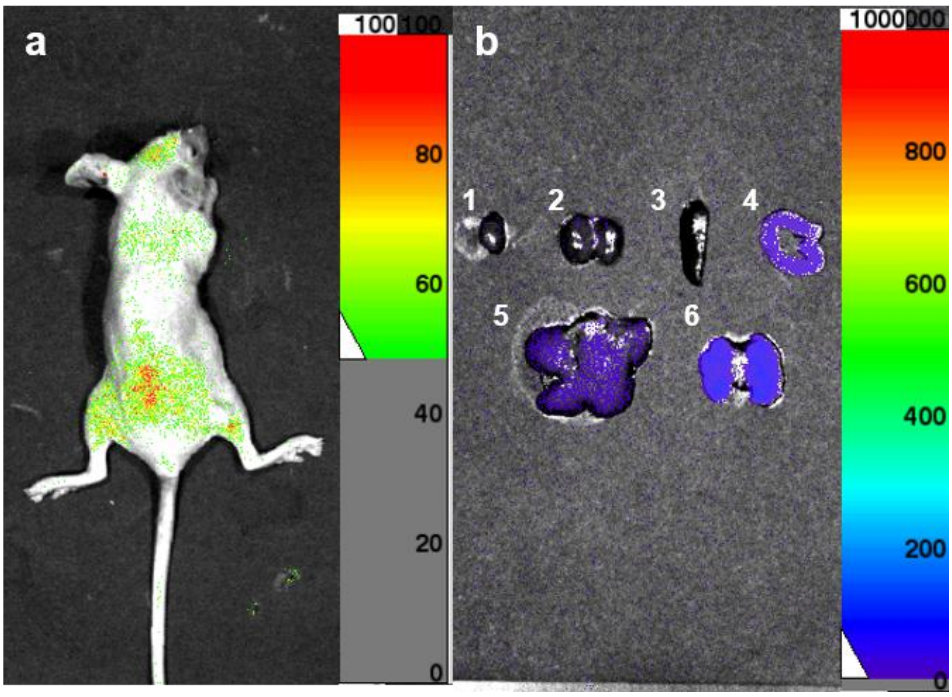


**Figure 9.** Determination of the biodistribution of CEs in nude mice (BALB/c-nu, 5 weeks) with **HBT-CE.** (a) Live fluorescence image taken from nude mice intravenously injected with 350 μL **HBT-CE** (200 μM). (b) Fluorescence image of ex vivo-dissected organs: (1) heart, (2) kidney, (3) spleen, (4) small intestine, (5) liver and (6) lung. All of the images were taken with an excitation laser at 365 nm and an

emission filter of 510 nm.

## Conclusion

A new strategy of probe-cavity matching was proposed to design a new fluorescent probe (**HBT-CE**) targeting CE isomers. **HBT-CE** showed a similar overall catalytic efficiency toward both CE isomers, with superior sensitivity and high specificity. It was also successfully applied to real-time monitoring of endogenous CEs in various cancer cell lines and live tracking of drug-induced CEs regulation. Furthermore, the *In Vivo* bioimaging ability of **HBT-CE** was demonstrated by sensing CE activity in living *zebrafish* and nude mice. The results reveal that **HBT-CE** could serve as a potential tool in CE-related drug discovery and disease diagnostics, as well as the functional study of drug metabolism and disease pathology.

## Acknowledgment

This work was funded by the National Key Research and Development Program of China (No. 2017YFA0505200), the National Natural Science Foundation of China (Nos. 21837001 and 21977036), and Hubei Province Natural Science Foundation (No. 2018CFA072).

## Supporting information

Probe characterization, HPLC analysis and additional data. This material is available free of charge via the Internet.

## References


(1) Satoh, T.; Hosokawa, M., Carboxylesterases: structure, function and polymorphism in mammals. *J. Pestic. Sci.* **2010,** *35*, 218-228.

(2) Mentlein, R.; Heymann, E., Hydrolysis of ester- and amide-type drugs by the purified isoenzymes of nonspecific carboxylesterase from rat liver. *Biochem. Pharmacol.* **1984,** *33*, 1243-1248.

(3) Furihata, T.; Hosokawa, M.; Fujii, A.; Derbel, M.; Satoh, T.; Chiba, K., Dexamethasone-induced methylprednisolone hemisuccinate hydrolase: its identification as a member of the rat carboxylesterase 2 family and its unique existence in plasma. *Biochem. Pharmacol.* **2005,** *69*, 1287-1297.

(4) Furihata, T.; Hosokawa, M.; Koyano, N.; Nakamura, T.; Satoh, T.; Chiba, K., Identification of di-(2-ethylhexyl) phthalate-induced carboxylesterase 1 in C57BL/6 mouse liver microsomes: purification, cDNA cloning, and baculovirus-mediated expression. *Drug Metab. Dispos.* **2004,** *32*, 1170-1177.

(5) Satoh, T.; Hosokawa, M., Structure, function and regulation of carboxylesterases. *Chem. Biol. Interact.* **2006,** *162*, 195-211.

(6) Hosokawa, M.; Maki, T.; Satoh, T., Characterization of molecular species of liver microsomal carboxylesterases of several animal species and humans. *Arch. Biochem. Biophys.* **1990,** *277*, 219-227.

(7) Fujita, K.; Kubota, Y.; Ishida, H.; Sasaki, Y., Irinotecan, a key chemotherapeutic drug for metastatic colorectal cancer. *World J. Gastroentero.* **2015,** *21*, 12234-12248.

(8) Capello, M.; Lee, M.; Wang, H.; Babel, I.; Katz, M. H.; Fleming, J. B.; Maitra, A.; Wang, H.; Tian, W.; Taguchi, A.; Hanash, S. M., Carboxylesterase 2 as a Determinant of Response to Irinotecan and Neoadjuvant FOLFIRINOX Therapy in Pancreatic Ductal Adenocarcinoma. *J. Natl. Cancer Inst.* **2015,** *107*, djv132.

(9) Uchida, K.; Otake, K.; Tanaka, K.; Hashimoto, K.; Saigusa, S.; Matsushita, K.; Koike, Y.; Inoue, M.; Ueeda, M.; Okugawa, Y.; Inoue, Y.; Mohri, Y.; Kusunoki, M., Clinical implications of CES2 RNA expression in neuroblastoma. *J. Pediatr.*

*Surg.* **2013,** *48*, 502-509.

(10) Ohtsuka, K.; Inoue, S.; Kameyama, M.; Kanetoshi, A.; Fujimoto, T.; Takaoka, K.; Araya, Y.; Shida, A., Intracellular conversion of irinotecan to its active form, SN-38, by native carboxylesterase in human non-small cell lung cancer. *Lung Cancer* **2003,** *41*, 187-198.

(11) Shaojun, C.; Li, H.; Haixin, H.; Guisheng, L., Expression of Topoisomerase 1 and carboxylesterase 2 correlates with irinotecan treatment response in metastatic colorectal cancer. *Cancer. Biol. Ther.* **2018,** *19*, 153-159.

(12) Ning, R.; Wang, X. P.; Zhan, Y. R.; Qi, Q.; Huang, X. F.; Hu, G.; Guo, Q. L.; Liu, W.; Yang, J., Gambogic acid potentiates clopidogrel-induced apoptosis and attenuates irinotecan-induced apoptosis through down-regulating human carboxylesterase 1 and -2. *Xenobiotica* **2016,** *46*, 816-824.

(13) von Hoff, D., Future directions for clinical research with CPT-11 (irinotecan). *Eur. J. Cancer.* **1996,** *32A Suppl 3*, S9-12.

(14) Hamzic, S.; Kummer, D.; Milesi, S.; Mueller, D.; Joerger, M.; Aebi, S.; Amstutz, U.; Largiader, C. R., Novel Genetic Variants in Carboxylesterase 1 Predict Severe Early-Onset Capecitabine-Related Toxicity. *Clin. Pharmacol. Ther.* **2017,** *102*, 796-804.

(15) Cho, M. K.; Lim, C. S.; Sarkar, A. R.; Lee, H. W.; Choi, H. J.; Noh, C. K.; Shin, S. J.; Kim, H. M., A two-photon ratiometric probe for detection of hNQO1 enzyme activity in human colon tissue. *Sensor Actuat B-Chem* **2018,** *272*, 203-210.

(16) Smith, G. C.; Kenna, J. G.; Harrison, D. J.; Tew, D.; Wolf, C. R., Autoantibodies to hepatic microsomal carboxylesterase in halothane hepatitis. *Lancet* **1993,** *342*, 963-964.

(17) Talcott, R. E.; Pond, S. M.; Ketterman, A.; Becker, C. E., Ethylesterases as indicators of liver damage I. Studies on malathion carboxylesterases. *Toxicol. Appl. Pharmacol.* **1982,** *65*, 69-74.

(18) Kálmán, A.; Kálmán, Z.; Velösy, G.; Vargha, G.; Vargha, G.; Papp, M., Activity of "nonspecific pancreatic carboxylesterase" in rat serum in experimentally

induced acute pancreatitis (preliminary results). *Acta Physiol. Hung.* **1989,** *73*, 315-317.

(19) Blind, P. J.; Buchler, M.; Blackberg, L.; Andersson, Y.; Uhl, W.; Beger, H. G.; Hernell, O., Carboxylic ester hydrolase. A sensitive serum marker and indicator of severity of acute pancreatitis. *Int. J. Pancreatol.* **1991,** *8*, 65-73.

(20) Ozkaya, A.; Sahin, Z.; Kuzu, M.; Saglam, Y. S.; Ozkaraca, M.; Uckun, M.; Yologlu, E.; Comakli, V.; Demirdag, R.; Yologlu, S., Role of geraniol against lead acetate-mediated hepatic damage and their interaction with liver carboxylesterase activity in rats. *Arch. Physiol. Biochem.* **2018,** *124*, 80-87.

(21) Liu, H. W.; Li, K.; Hu, X. X.; Zhu, L.; Rong, Q.; Liu, Y.; Zhang, X. B.; Hasserodt, J.; Qu, F. L.; Tan, W., In Situ Localization of Enzyme Activity in Live Cells by a Molecular Probe Releasing a Precipitating Fluorochrome. *Angew. Chem. Int. Ed.* **2017,** *56*, 11788-11792.

(22) Sedgwick, A. C.; Wu, L.; Han, H. H.; Bull, S. D.; He, X. P.; James, T. D.; Sessler, J. L.; Tang, B. Z.; Tian, H.; Yoon, J., Excited-state intramolecular proton-transfer (ESIPT) based fluorescence sensors and imaging agents. *Chem. Soc. Rev.* **2018,** *47*, 8842-8880.

(23) Rathore, B.; Sunwoo, K.; Jangili, P.; Kim, J.; Kim, J. H.; Huang, M.; Xiong, J.; Sharma, A.; Yang, Z.; Qu, J.; Kim, J. S., Nanomaterial designing strategies related to cell lysosome and their biomedical applications: A review. *Biomaterials* **2019,** *211*, 25-47.

(24) Li, H.; Li, Y.; Yao, Q.; Fan, J.; Sun, W.; Long, S.; Shao, K.; Du, J.; Wang, J.; Peng, X., In situ imaging of aminopeptidase N activity in hepatocellular carcinoma: a migration model for tumour using an activatable two-photon NIR fluorescent probe. *Chem. Sci.* **2019,** *10*, 1619-1625.

(25) Wu, X.; Shi, W.; Li, X.; Ma, H., Recognition Moieties of Small Molecular Fluorescent Probes for Bioimaging of Enzymes. *Acc. Chem. Res.* **2019,** *52*, 1892-1904.

(26) Wang, X.; Li, P.; Ding, Q.; Wu, C.; Zhang, W.; Tang, B., Observation of Acetylcholinesterase in Stress-Induced Depression Phenotypes by Two-Photon

Fluorescence Imaging in the Mouse Brain. *J. Am. Chem. Soc.* **2019,** *141*, 2061-2068.

(27) Li, Z.; Ren, M.; Wang, L.; Dai, L.; Lin, W., Development of a two-photon fluorescent probe for the selective detection of β-galactosidase in living cells and tissues. *J. Mater. Chem. B* **2019,** *7*, 3431-3437.

(28) Zhang, Y.; Chen, W.; Feng, D.; Shi, W.; Li, X.; Ma, H., A spectroscopic off-on probe for simple and sensitive detection of carboxylesterase activity and its application to cell imaging. *Analyst* **2012,** *137*, 716-721.

(29) Park, S. J.; Lee, H. W.; Kim, H. R.; Kang, C.; Kim, H. M., A carboxylesterase-selective ratiometric fluorescent two-photon probe and its application to hepatocytes and liver tissues. *Chem. Sci.* **2016,** *7*, 3703-3709.

(30) Zhou, H.; Tang, J.; Zhang, J.; Chen, B.; Kan, J.; Zhang, W.; Zhou, J.; Ma, H., A red lysosome-targeted fluorescent probe for carboxylesterase detection and bioimaging. *J. Mater. Chem. B* **2019,** *7*, 2989-2996.

(31) Wang, J.; Chen, Q.; Tian, N.; Zhu, W.; Zou, H.; Wang, X.; Li, X.; Fan, X.; Jiang, G.; Tang, B. Z., A fast responsive, highly selective and light-up fluorescent probe for the two-photon imaging of carboxylesterase in living cells. *J. Mater. Chem. B* **2018,** *6*, 1595-1599.

(32) Gao, M.; Hu, Q.; Feng, G.; Tang, B. Z.; Liu, B., A fluorescent light-up probe with "AIE + ESIPT" characteristics for specific detection of lysosomal esterase. *J. Mater. Chem. B* **2014,** *2*, 3438-3442.

(33) Li, D.; Li, Z.; Chen, W.; Yang, X., Imaging and Detection of Carboxylesterase in Living Cells and Zebrafish Pretreated with Pesticides by a New Near-Infrared Fluorescence Off-On Probe. *J. Agric. Food Chem.* **2017,** *65*, 4209-4215.

(34) Li, M.; Zhai, C.; Wang, S.; Huang, W.; Liu, Y.; Li, Z., Detection of carboxylesterase by a novel hydrosoluble near-infrared fluorescence probe. *RSC Adv.* **2019,** *9*, 40689-40693.

(35) Nicolet, Y.; Lockridge, O.; Masson, P.; Fontecilla-Camps, J. C.; Nachon, F., Crystal structure of human butyrylcholinesterase and of its complexes with substrate and products. *J. Biol. Chem.* **2003,** *278*, 41141-41147.

(36) Bencharit, S.; Morton, C. L.; Xue, Y.; Potter, P. M.; Redinbo, M. R., Structural basis of heroin and cocaine metabolism by a promiscuous human drug-processing enzyme. *Nat. Struct. Biol.* **2003,** *10*, 349-356.

(37) Ahowesso, C.; Piccolo, E.; Li, X. M.; Dulong, S.; Hossard, V.; La Sorda, R.; Filipski, E.; Tinari, N.; Delaunay, F.; Iacobelli, S.; Levi, F., Relations between strain and gender dependencies of irinotecan toxicity and UGT1A1, CES2 and TOP1 expressions in mice. *Toxicol. Lett.* **2010,** *192*, 395-401.

(38) Zhu, H. J.; Wang, X.; Gawronski, B. E.; Brinda, B. J.; Angiolillo, D. J.; Markowitz, J. S., Carboxylesterase 1 as a determinant of clopidogrel metabolism and activation. *J. Pharmacol. Exp. Ther.* **2013,** *344*, 665-672.

(39) Ding, L.; Tian, Z.; Hou, J.; Dou, T.; Jin, Q.; Wang, D.; Zou, L.; Zhu, Y.; Song, Y.; Cui, J.; Ge, G., Sensing carboxylesterase 1 in living systems by a practical and isoform-specific fluorescent probe. *Chinese Chem. Lett.* **2019,** *30*, 558-562.

(40) Chen, K. F.; Chen, H. L.; Tai, W. T.; Feng, W. C.; Hsu, C. H.; Chen, P. J.; Cheng, A. L., Activation of phosphatidylinositol 3-kinase/Akt signaling pathway mediates acquired resistance to sorafenib in hepatocellular carcinoma cells. *J. Pharmacol. Exp. Ther.* **2011,** *337*, 155-161.

(41) Toffoli, G.; Cecchin, E.; Gasparini, G.; D'Andrea, M.; Azzarello, G.; Basso, U.; Mini, E.; Pessa, S.; De Mattia, E.; Lo Re, G.; Buonadonna, A.; Nobili, S.; De Paoli, P.; Innocenti, F., Genotype-driven phase I study of irinotecan administered in combination with fluorouracil/leucovorin in patients with metastatic colorectal cancer. *J. Clin. Oncol.* **2010,** *28*, 866-871.

(42) Tamura, T.; Kuwahara, A.; Kadoyama, K.; Yamamori, M.; Nishiguchi, K.; Inokuma, T.; Takemoto, Y.; Chayahara, N.; Okuno, T.; Miki, I.; Fujishima, Y.; Sakaeda, T., Effects of bolus injection of 5-fluorouracil on steady-state plasma concentrations of 5-fluorouracil in Japanese patients with advanced colorectal cancer. *Int. J. Med. Sci.* **2011,** *8*, 406-412.

(43) Yamashita, K.; Nagashima, F.; Fujita, K.; Yamamoto, W.; Endo, H.; Miya, T.; Narabayashi, M.; Kawara, K.; Akiyama, Y.; Ando, Y.; Ando, M.; Sasaki, Y., Phase I/II study of FOLFIRI in Japanese patients with advanced colorectal

cancer. *Jpn. J. Clin. Oncol.* **2011,** *41*, 204-209.

(44) Shang, W.; Liu, J.; Chen, R.; Ning, R.; Xiong, J.; Liu, W.; Mao, Z.; Hu, G.; Yang, J., Fluoxetine reduces CES1, CES2, and CYP3A4 expression through decreasing PXR and increasing DEC1 in HepG2 cells. *Xenobiotica* **2016,** *46*, 393-405.

(45) Kuster, E., Cholin- and carboxylesterase activities in developing zebrafish embryos (Danio rerio) and their potential use for insecticide hazard assessment. *Aquat. Toxicol.* **2005,** *75*, 76-85.

(46) Zhou, Z.; Wang, F.; Yang, G.; Lu, C.; Nie, J.; Chen, Z.; Ren, J.; Sun, Q.; Zhao, C.; Zhu, W. H., A Ratiometric Fluorescent Probe for Monitoring Leucine Aminopeptidase in Living Cells and Zebrafish Model. *Anal. Chem.* **2017,** *89*, 11576-11582.

(47) Liu, S. Y.; Xiong, H.; Yang, J. Q.; Yang, S. H.; Li, Y.; Yang, W. C.; Yang, G. F., Discovery of Butyrylcholinesterase-Activated Near-Infrared Fluorogenic Probe for Live-Cell and In Vivo Imaging. *ACS Sens.* **2018,** *3*, 2118-2128.

(48) Jin, Q.; Feng, L.; Wang, D. D.; Wu, J. J.; Hou, J.; Dai, Z. R.; Sun, S. G.; Wang, J. Y.; Ge, G. B.; Cui, J. N.; Yang, L., A highly selective near-infrared fluorescent probe for carboxylesterase 2 and its bioimaging applications in living cells and animals. *Biosens. Bioelectron.* **2016,** *83*, 193-199.

(49) Satoh, T.; Taylor, P.; Bosron, W. F.; Sanghani, S. P.; Hosokawa, M.; La Du, B. N., Current progress on esterases: from molecular structure to function. *Drug Metab. Dispos.* **2002,** *30*, 488-493.

TOC

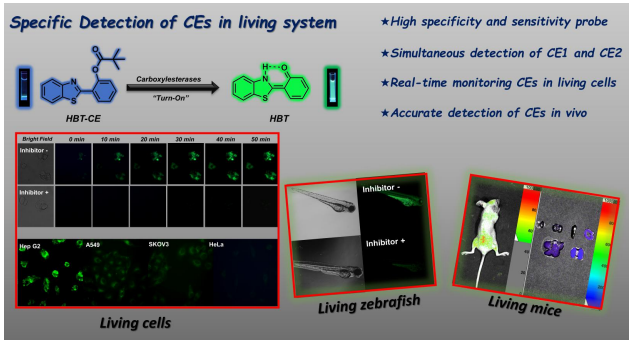
Specific Detection of CEs in living system
★High specificity and sensitivity probe
★Simultaneous detection of CE1 and CE2
★Real-time monitoring CEs in living cells
★Accurate detection of CEs in vivo
Carboxylesterases
"Turn-On"
HBT-CE
HBT
Living cells
Living zebrafish
Living mice